Hindawi
Geofluids
Volume 2021, Article ID 9975296, 15 pages
https://doi.org/10.1155/2021/9975296

Research Article

Numerical Simulation and Modeling on CO_2 Sequestration Coupled with Enhanced Gas Recovery in Shale Gas Reservoirs

Jie Zhan,[1,2] **Zhihao Niu**,[1,2] **Mengmeng Li**,[1,2] **Ying Zhang**,[3] **Xianlin Ma**,[1,2] **Chao Fan**,[1,2] **and Ruifei Wang**[1,2]

[1]*School of Petroleum Engineering, Xi'an Shiyou University, Xi'an 710065, China*
[2]*Engineering Research Center of Development and Management for Low to Ultra-Low Permeability Oil & Gas Reservoirs in West China, Ministry of Education, Xi'an Shiyou University, Xi'an 710065, China*
[3]*Natural Gas Engineering Design Department, Xi'an Changqing Technology Engineering Co. Ltd, Xi'an 710018, China*

Correspondence should be addressed to Jie Zhan; zhanjie@xsyu.edu.cn

Received 4 March 2021; Accepted 19 July 2021; Published 4 August 2021

Academic Editor: Sohrab Zendehboudi

CO_2 geological sequestration in shale is a promising method to mitigate global warming caused by greenhouse gas emissions as well as to enhance the gas recovery to some degree, which effectively addresses the problems related to energy demand and climate change. With the data from the New Albany Shale in the Illinois Basin in the United States, the CMG-GEM simulator is applied to establish a numerical model to evaluate the feasibility of CO_2 sequestration in shale gas reservoirs with potential enhanced gas recovery (EGR). To represent the matrix, natural fractures, and hydraulic fractures in shale gas reservoirs, a multicontinua porous medium model will be developed. Darcy's and Forchheimer's models and desorption-adsorption models with a mixing rule will be incorporated into the multicontinua numerical model to depict the three-stage flow mechanism, including convective gas flow mainly in fractures, dispersive gas transport in macropores, and CH_4-CO_2 competitive sorption phenomenon in micropores. With the established shale reservoir model, different CO_2 injection schemes (continuous injection vs. pulse injection) for CO_2 sequestration in shale gas reservoirs are investigated. Meanwhile, a sensitivity analysis of the reservoir permeability between the hydraulic fractures of production and injection wells is conducted to quantify its influence on reservoir performance. The permeability multipliers are 10, 100, and 1,000 for the sensitivity study. The results indicate that CO_2 can be effectively sequestered in shale reservoirs. But the EGR of both injection schemes does not perform well as expected. In the field application, it is necessary to take the efficiency of supplemental energy utilization, the CO_2 sequestration ratio, and the effect of injected CO_2 on the purity of produced methane into consideration to design an optimal execution plan. The case with a permeability multiplier of 1,000 meets the demand for both CO_2 sequestration and EGR, which indicates that a moderate secondary stimulation zone needs to be formed between the primary hydraulic fractures of injection and production wells to facilitate the efficient energy transfer between interwell as well as to prevent CO_2 from channeling. To meet the demand for CO_2 sequestration in shale gas reservoirs with EGR, advanced and effective fracking is essential.

1. Introduction

At present, fossil fuels are the primary source of energy consumption in the world [1–3], which leads to abundant CO_2 being released into the atmosphere via the combustion of fossil fuels (oil, natural gas, and coal). Before the industrial revolution, the average concentration of CO_2 in the atmosphere was 0.03%, which has increased to 0.04% in 2005 and is expected to reach 0.01% by 2100 without any intervention [4–6]. The release of huge amounts of CO_2 into the atmosphere leads to global warming and ocean acidification, which will be harmful to the whole world. Therefore, mitigating the contribution of CO_2 emissions to global warming has become a common problem faced by all the countries. It is expected that China's total CO_2 emissions will reach 67×10^8 t in 2030 and surpass the United States, to become the world's largest CO_2 emitter [7, 8]. CCS, as an emerging technology, is expected to play a key role in CO_2 emission

reduction [9, 10]. From 2010 to 2050, 14% of the CO_2 emission reduction arises from the application of CCS, making it the largest contributor to GHG emission reduction [11].

With the booming of commercial shale gas development, many researchers focus on the feasibility study of CO_2 sequestration in shale gas reservoirs with enhanced gas recovery [12–14]. Based on different shale samples, several researchers have extensively studied the interaction between CO_2 and CH_4 in shales. Nuttal et al. [15] systematically investigated the sorption capacity of CH_4 and CO_2 in the Ohio Shale of the Upper Devonian in eastern Kentucky. And the results indicated that the organic matter of the Ohio black shale has a complex microporous structure similar to the coal, which can facilitate the adsorption of large amounts of gas. With organic-rich shale samples from the Fort Worth Basin, Kang et al. [16] tested the sorption capacity for CO_2 and CH_4. The lab data demonstrated that 40% more CO_2 was preferentially adsorbed. Compared to CH_4, the preferential sorption of CO_2 by shale is beneficial for the enhanced recovery of shale gas with the CO_2 injection while effectively sequestering a certain amount of CO_2. But the actual reservoir performance is highly related to the reservoir geological conditions and engineering parameters. Godec et al. [17] showed that the primary recovery of shale gas in the Marcellus Shale reservoir or shale reservoirs similar to the Marcellus Shale is 20%-35%, with an average recovery of 25%. With an appropriate well spacing between injector and producer, 7% of recovery increment can be obtained with the CO_2 injection. Zhang [18] conducted in-house experiments on CO_2 injection enhancing shale gas recovery for terrestrial shale samples from Fuxian of Ordos Basin. The lab results showed that the recovery of CO_2 injection is 80.29%, 7.66% higher compared to the depleted development.

However, as to the Devonian and Mississippian Shales in the Illinois Basin and the Silurian Ohio Shale in eastern Kentucky, the EGR with CO_2 injection does not perform well as expected, with a recovery increment less than 1%. In the case of Devonian and Mississippian Shales, the energy transfer efficiency is impeded by the tight and unstimulated matrix between the hydraulic fractures of the injector and producer. In the case of Ohio Shale, the reservoir pressure is still high while injecting CO_2, limiting the amount of CO_2 injection and the corresponding shale gas recovery. In China, there are some CCS projects on CO_2 sequestration in depleted oil reservoirs or saline aquifers, such as the Shenhua Ordos pilot-scale project for CO_2 deep saline aquifer storage [19]. The CS-EGR in shale reservoirs is still in the preliminary stage even with abundant shale resources [20]. But the CS-EGR in shale reservoirs has attracted extensive attention recently in China [21, 22]. There are still many challenges to prove the viability of sequestration and enhanced recovery in shale reservoirs because of the complicated mechanisms of the process and the engineering complexity of CO_2 injection in shale reservoirs.

In the paper, to objectively evaluate the feasibility of CO_2 sequestration in shale gas reservoirs with potential enhanced gas recovery (EGR), numerical simulation studies are carried out to investigate the mechanism of the process and the effects of several dominating engineering parameters on the reservoir performance to explore the engineering complexity of CO_2 injection in shale reservoirs, taking the New Albany Shale as an example. A multicontinua porous medium model will be developed to represent the domains (matrix, natural fractures, and hydraulic fractures) in shale gas reservoirs. A different domain has its own scale and corresponding transport mechanism. Darcy's and Forchheimer's models and desorption-adsorption models with a mixing rule will be incorporated into the multicontinua numerical model to mimic gas migration in different domains. The gridding scheme, local grid refinement with logarithmic spacing, is employed to accurately simulate the detailed transient gas flow phenomenon around hydraulic fractures. With the established shale reservoir model, different CO_2 injection schemes (continuous injection vs. pulse injection) for CO_2 sequestration in shale gas reservoirs are investigated. Meanwhile, a sensitivity analysis of the reservoir permeability between the hydraulic fractures of the producer and injector is conducted to quantify its influence on reservoir performance. The insights obtained from the study will not only improve the understanding of CO_2 sequestration in shale reservoirs but also provide new methods for enhancing shale gas recovery, which effectively promotes the technology development and wide application of CCS in China and across the world.

2. Reservoir Model and Simulation Schemes

2.1. Overview of the New Albany Shale. The volumes of original gas-in-place (OGIP) and technically recoverable gas in the New Albany Shale are estimated to be $2.43–4.52 \times 10^{12}$ m^3 and $5.4–54.3 \times 10^{10}$ m^3. The New Albany Shale lies at a relatively shallow depth, from 0 to 1524 m [23]. It is 30.5–42.7 m thick in southeastern Indiana and dips and thickens to the southwest into the Illinois Basin, where it reaches a thickness of more than 140.2 m near the intersection of Illinois, Indiana, and Kentucky (Figure 1).

2.2. Numerical Simulation Methodology. With the data from the New Albany Shale, the CMG-GEM simulator is implemented to establish a reservoir model. The governing equations employed in the CMG's general EOS compositional simulator (GEM), which depicts the total mass balance for each component including accumulation term as well as convection term and sink/source term, are expressed by the continuity equations below [24]:

$$\frac{\partial(\varnothing \rho_w S_w)}{\partial t} = -\nabla \cdot (\rho_w v_w) + q_w,$$
$$\frac{\partial\left(\varnothing\left(y_i \rho_g S_g + x_i \rho_o S_o\right)\right)}{\partial t} = -\nabla \cdot \left(y_i \rho_g v_g + x_i \rho_o v_o\right) + q_i, \quad (1)$$

where $\rho_{k=o,\,g,w}$ denotes the density of phase k, where k represents the phases (o is oil phase, g is gas phase, and w is water phase); $v_{k=o,\,g,w}$ is Darcy's flow velocity of each phase; $s_{k=o,\,g,w}$ is the saturation of each phase; y_i is the mole fraction of

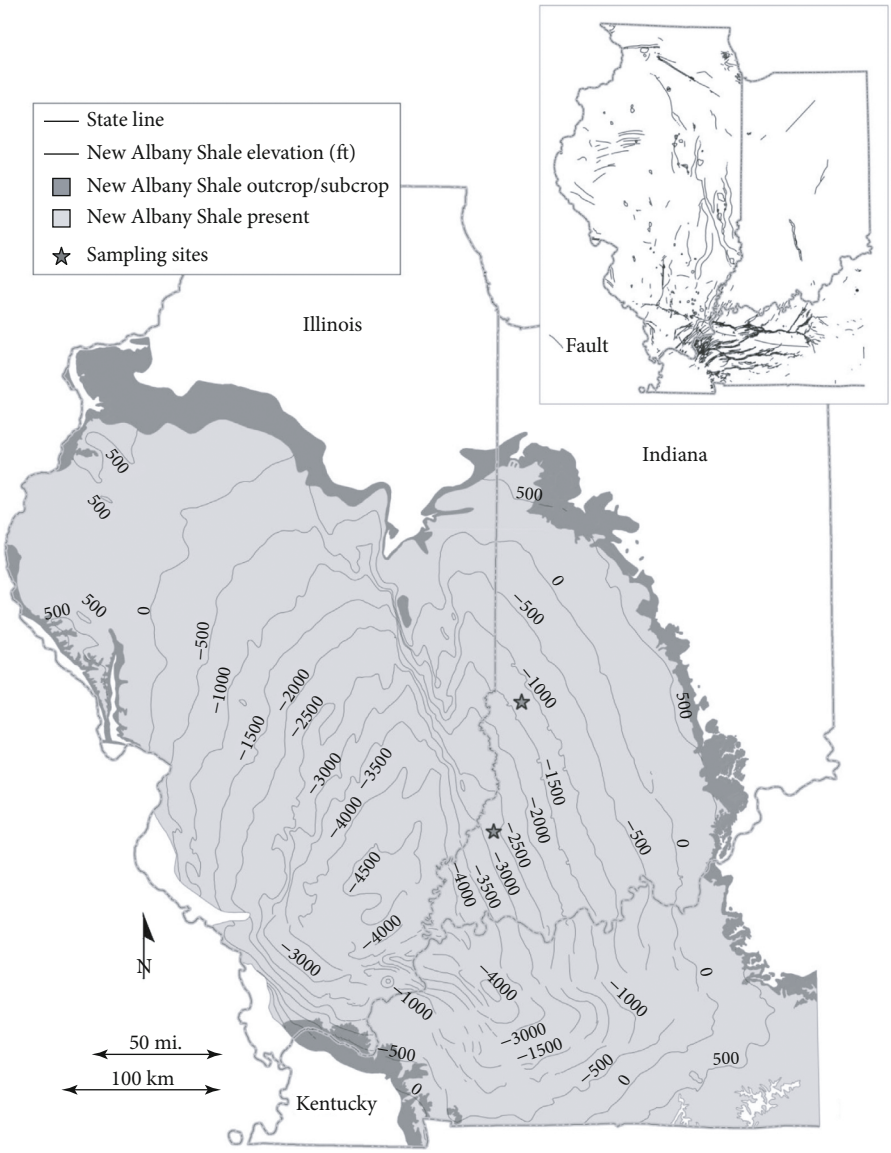

(a)

Figure 1: Continued.

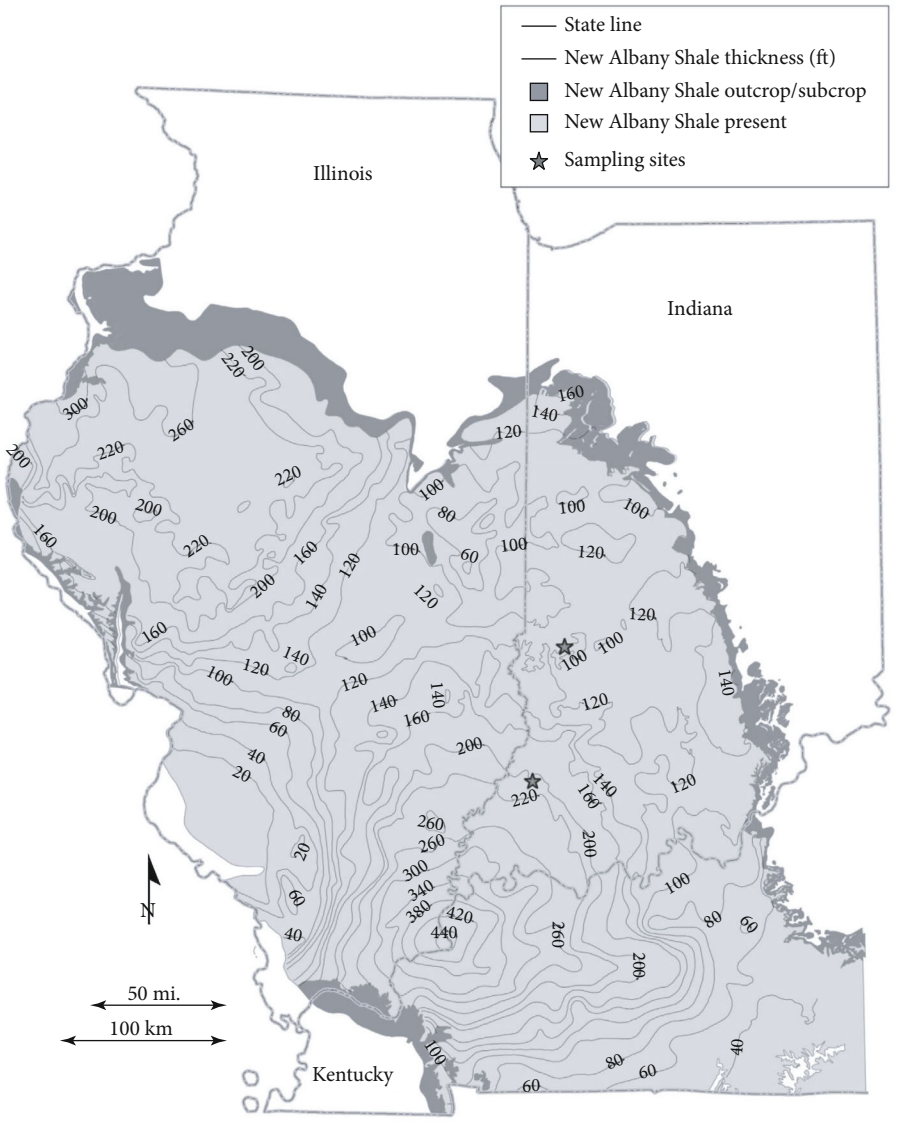

(b)

Figure 1: (a) New Albany Shale elevation in the Illinois Basin; (b) New Albany Shale extent and thickness in the Illinois Basin [23].

component i in the gas phase; x_i is the mole fraction of component i in the oil phase; $\varnothing$ is the porosity; and q_i denotes the injection/production of component i.

To meet the needs of thermodynamic equilibrium, the Peng-Robinson equation of state is generally applied in the GEM to determine the component composition and compressibility factor for each phase.

The Langmuir isotherm has been widely employed to simulate single component adsorption:

$$V(P) = \frac{V_{\mathrm{L}}\mathrm{P}}{P + P_{\mathrm{L}}}, \tag{2}$$

where $V(P)$ is the gas volume of adsorption at pressure P; V_{L} is the Langmuir volume, referred to as the maximum adsorbed gas volume at the infinite pressure; and P_{L} is the Langmuir pressure, representing the pressure corresponding to a one-half Langmuir volume.

For modeling the competitive multicomponent adsorption-desorption process, an extended Langmuir isotherm is implemented [25]:

$$w_i = \frac{w_{i,\max} B_i y_{ig} P}{1 + \sum_j B_j y_{jg}}, \tag{3}$$

where w_i is the moles of adsorbed component i per unit mass or rock; $w_{i,\max}$ is the maximum moles of adsorbed component i per unit mass or rock; B_i is the parameter for Langmuir isotherm relation; P is the pressure; and y_{ig} is the molar fraction of adsorbed component i in the gas phase.

Both B_i and $\omega_{i,\max}$ are parameters of the Langmuir isotherm for single component i (CH_4 and CO_2), which are determined in the lab with the New Albany Shale samples.

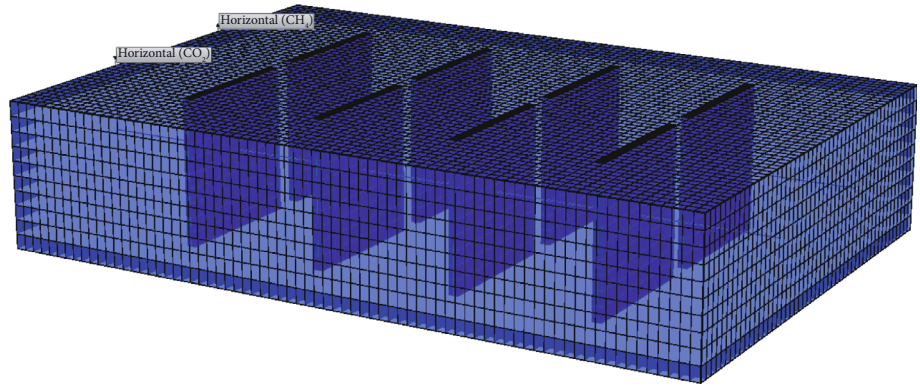

Figure 2: Three-dimensional model of the whole reservoir.

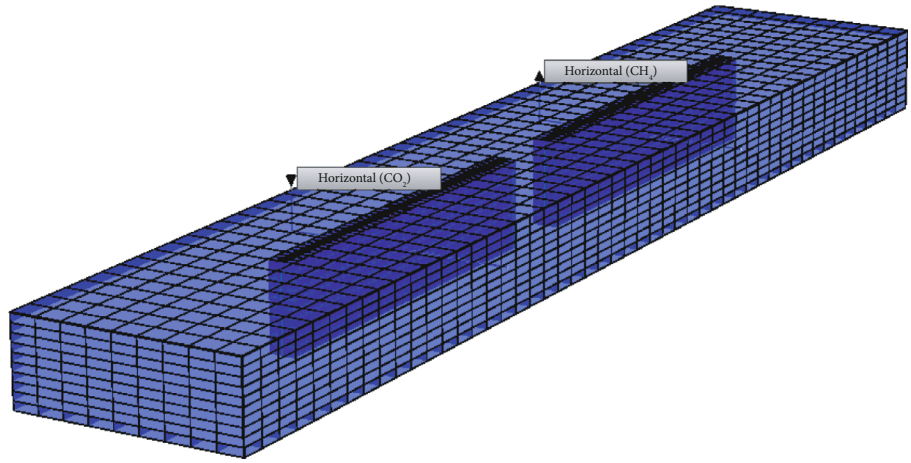

Figure 3: Three-dimensional submodel.

For the simulation of shale reservoirs developed with multistage hydraulic fractured horizontal wells, some more equations or models are applied to address the specialty. By implementing the correlation proposed by Evan and Civan, the Forchheimer model with the non-Darcy beta factor can be utilized to simulate a turbulent gas flow within hydraulic fractures, accounting for the inertial effects on the flow characteristics [26]:

$$-\nabla P = \frac{\mu}{K} v + \beta \rho v^2, \qquad \beta = \frac{1.485E9}{K^{1.021}}, \tag{4}$$

where v is the velocity, K is the permeability, μ is the viscosity, ρ is the density, P is the pressure, and β is the non-Darcy beta factor, determined by the correlation proposed by Evan and Civan.

Local grid refinement with logarithmic spacing, which discretizes the reservoir to a finer degree region around hydraulic fractures and more coarsely further away from the hydraulic fractures, is implemented to accurately depict the detailed transient gas flow phenomenon around the hydraulic fractures. A dual-permeability model is employed to take natural fractures acting as boundaries to matrix elements in three directions into consideration, where the governing equations of the dual-permeability model are an extension of the equations for single porosity systems. There are two sets of mass balance equations, with one for the matrix system and the other one for the natural fracture system. Meanwhile, new terms, accounting for the matrix-

Table 1: List of model parameters.

Depth (m)	420
Thickness (m)	30.5
Matrix porosity	3.4%
Fracture porosity	0.1%
Matrix permeability (mD)	0.00015
Fracture permeability (mD)	0.004
Rock density ($g \cdot cm^{-3}$)	2.4
Maximum adsorption mass CH_4 ($m^3 \cdot ton^{-1}$)	3.3
Langmuir adsorption constant CH_4 ($1 \cdot Pa^{-1}$)	0.00016
Maximum adsorption mass CO_2 ($m^3 \cdot ton^{-1}$)	14.3
Langmuir adsorption constant CO_2 ($1 \cdot Pa^{-1}$)	0.00013
Horizontal well length (m)	1,537.4
Hydraulic fracture conductivity (mD·m)	6,100
Half-length of hydraulic fracture (m)	137.2

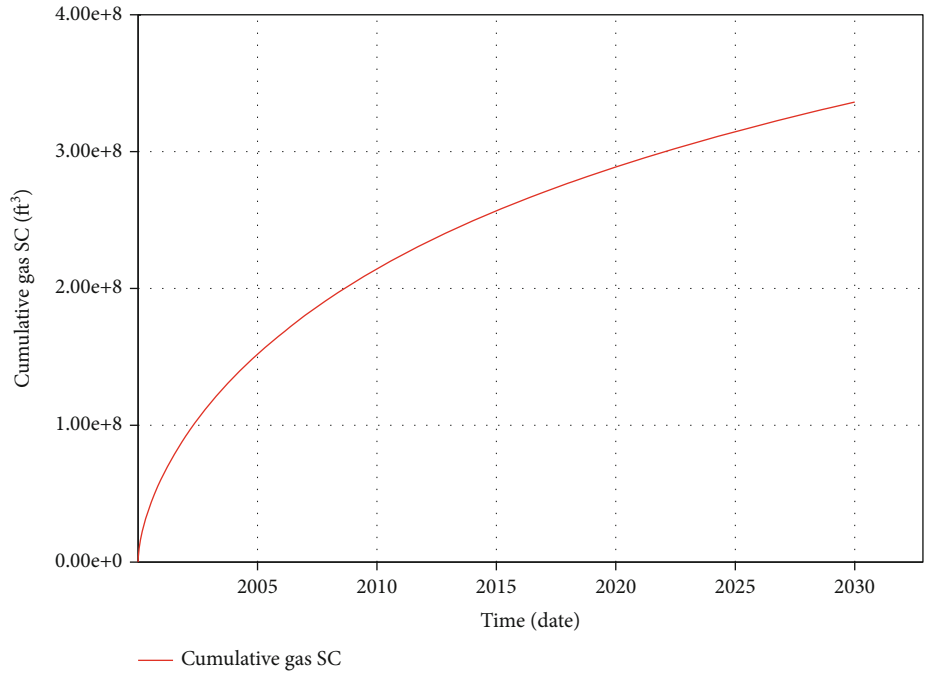

Figure 4: Simulation results of scheme 1: cumulative gas production.

fracture transfer in each phase for each component, are included in the mass balance equations of the dual-permeability model. The logarithmically spaced, locally refined, and dual permeability (LS-LR-DK) methodology has been widely applied to simulate gas flows in hydraulically fractured shale gas reservoirs, which has been validated by previous work to both accurately and efficiently simulate stimulated fractured shale reservoirs [23, 27, 28].

2.3. Reservoir Model. Based on the CMG-GEM simulator, a homogeneous 3D multicontinua porous medium model is developed to evaluate the feasibility of CO_2 sequestration in shale gas reservoirs with potential enhanced gas recovery (EGR). The dimensions of the numerical model are 1445 m $\times$ 914 m $\times$ 30 m, corresponding to the length, width, and thickness of the shale gas reservoir, respectively, as shown in Figure 2. Two horizontal wells are simulated with four fracturing stages each, upon which each fracturing stage has a single perforated interval. The local grid refinement with logarithmic spacing is employed to model hydraulic fractures explicitly in the matrix portion by defining high permeability values for the hydraulic fractures and low permeability values for the shale matrix. The competitive CH_4–CO_2 adsorption-desorption is simulated based on the extended Langmuir model.

Due to expensive computational time and cost for the entire field case, in the study, a submodel with one fracking stage for each horizontal well is extracted from the whole reservoir model. The dimensions of the submodel are 164.6 m $\times$ 914.4 m $\times$ 30.5 m, as shown in Figure 3. The entire simulation period is 30 years. First of all, the shale reservoir is depleted for five years. Methane is recovered from the CH_4 producer drilled in the shale reservoir with a maximum gas rate at a surface condition (STG) of 2.8×10^4 m^3/day and minimum bottom-hole pressure (BHP) of 1379 kPa. With a constant daily injection rate of 1.1×10^3 m^3/day, CO_2 is injected by continuous and pulsed injection, respectively. The injection time is 5 years. The specific parameters used in the numerical model are listed in Table 1.

2.4. Simulation Schemes. With the established shale reservoir model, different CO_2 injection schemes (continuous injection vs. pulse injection) for CO_2 sequestration in shale gas reservoirs are investigated. The following three schemes are simulated. Scheme 1 is a depletion development scheme without CO_2 injection. In scheme 2 and scheme 3, CO_2 is injected from the 5th year to the 10th year. Scheme 2 is continuous injection, and scheme 3 is pulse injection.

Scheme 1: depletion development. Based on this scheme, 9.52×10^6 m^3 of CH_4 is produced over 30 years, as shown in Figure 4.

Scheme 2: continuous injection. In scheme 2, CO_2 is injected continuously from the 5th year to the 10th year. During the five-year injection, the cumulative injection of CO_2 is 2.07×10^6 m^3 through the one-stage hydraulic fracture. And the total gas production is 9.56×10^6 m^3 at the end of the simulation. The gas production of each component is CH_4 (9.31×10^6 m^3) and CO_2 (0.25×10^6 m^3), respectively, as shown in Figure 5. The reservoir pressure is improved by CO_2 injection, resulting in higher total gas production. Compared to scheme 1, the decrease of CH_4 production of scheme 2 is due to the change of composition by CO_2 injection, reducing the purity of produced methane. The EGR of the scheme does not perform well as expected. Most of the supplemental energy is trapped around an injector due to a tight formation impeding the effective pressure communications between an injector and a producer, dominating the success of the EGR, as shown in Figure 6(a). That is

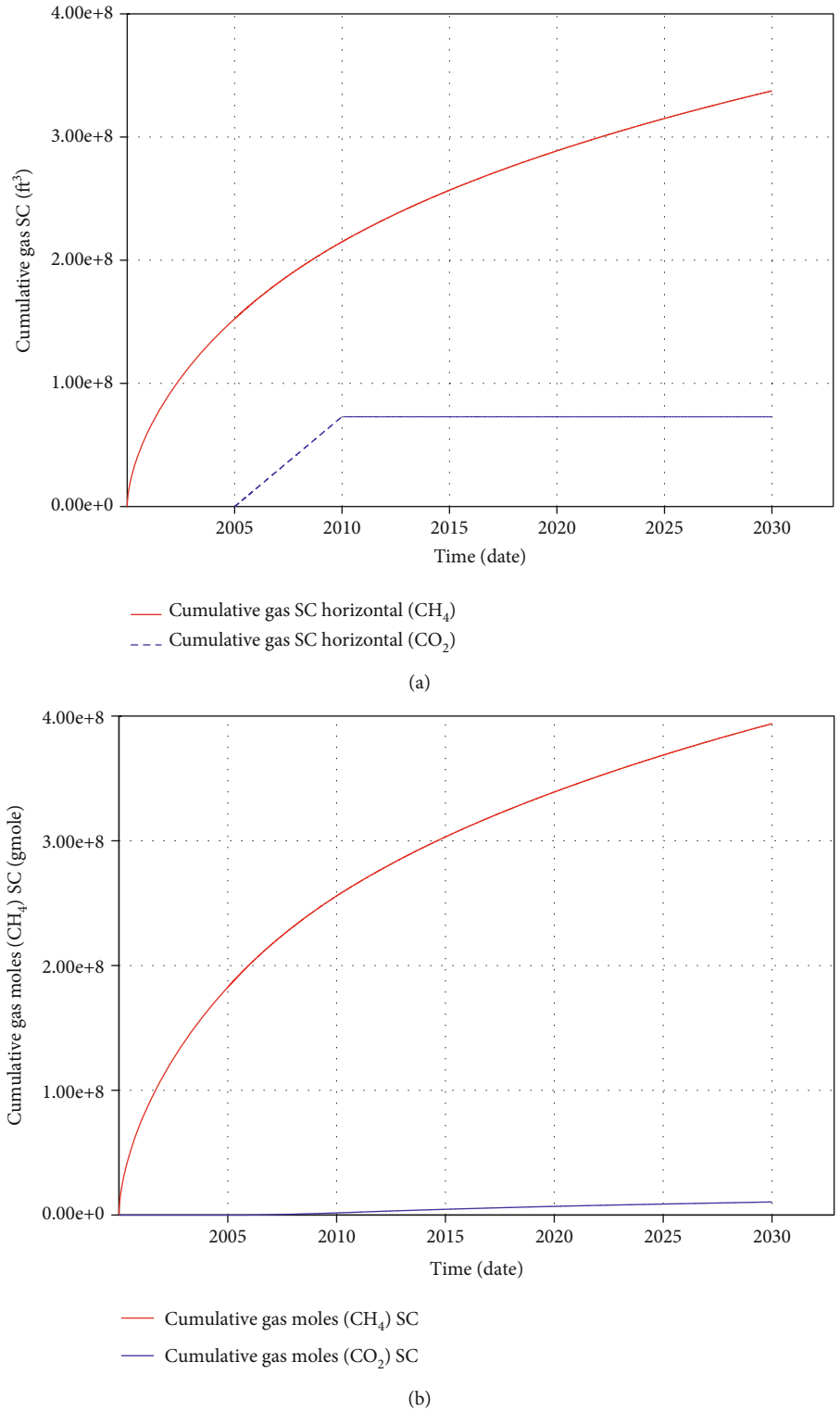

Figure 5: (a) Simulation results of scheme 2: cumulative gas production, CO_2 injection; (b) cumulative production of each component.

why the reservoir productivity is enhanced by the injection process. But the increment is not substantial. Overall, the supplemental energy is not effectively utilized to offset the impact of CO_2 injection on the purity of produced methane. But the injected CO_2 is effectively sequestered. At the end of the 30-year simulation, 87.9% of CO_2 is still effectively sequestered in shale reservoirs.

Scheme 3: pulse injection. In scheme 3, CO_2 is injected by pulse injection from the 5th year to the 10th year, pulse injection starting from the first month of the 5th year, with CO_2

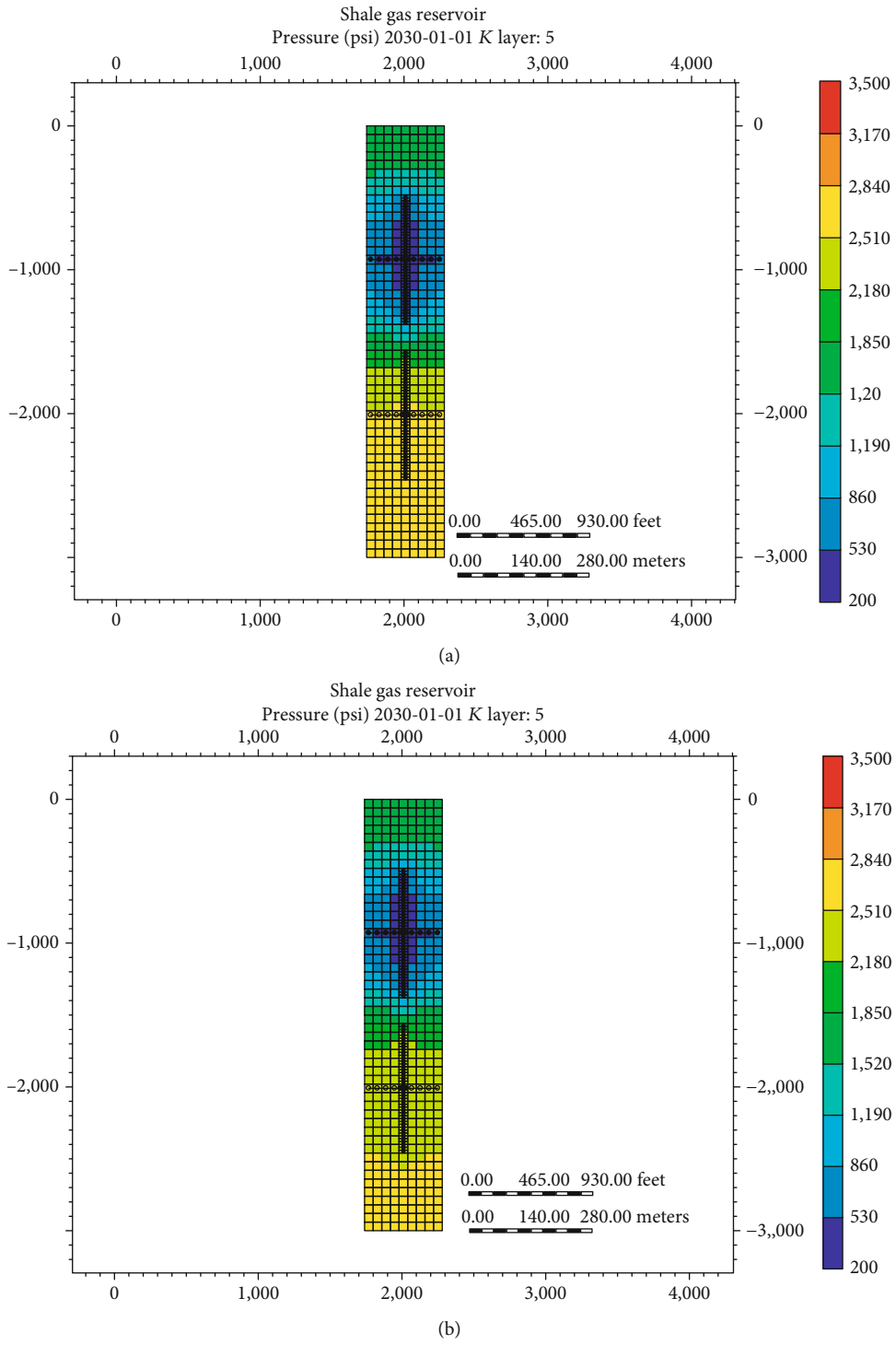

Figure 6: Pressure distribution: (a) scheme 2; (b) scheme 3.

injection for one month and then shutting in for one month repeatedly throughout the 5 years. During the five years, 1.04×10^6 m^3 of CO_2 is injected through the hydraulic fracture. And the total gas production is 9.53×10^6 m^3. The gas production of each component is CH_4 (9.33×10^6 m^3) and CO_2 (0.20×10^6 m^3), as shown in Figure 7. Like scheme 2, injected CO_2 is effectively sequestered. At the end of the 30-year simulation, 80.8% of CO_2 is still effectively sequestered in the shale reservoir. With the CO_2 injection at half the amount of scheme 2, the total gas production of scheme 3 is basically the same as scheme 2 with the difference of 0.03 $\times 10^6$ m^3. The difference in total gas production between scheme 2 and scheme 3 is small, mainly due to the low efficiency of supplemental energy utilization. Most of the

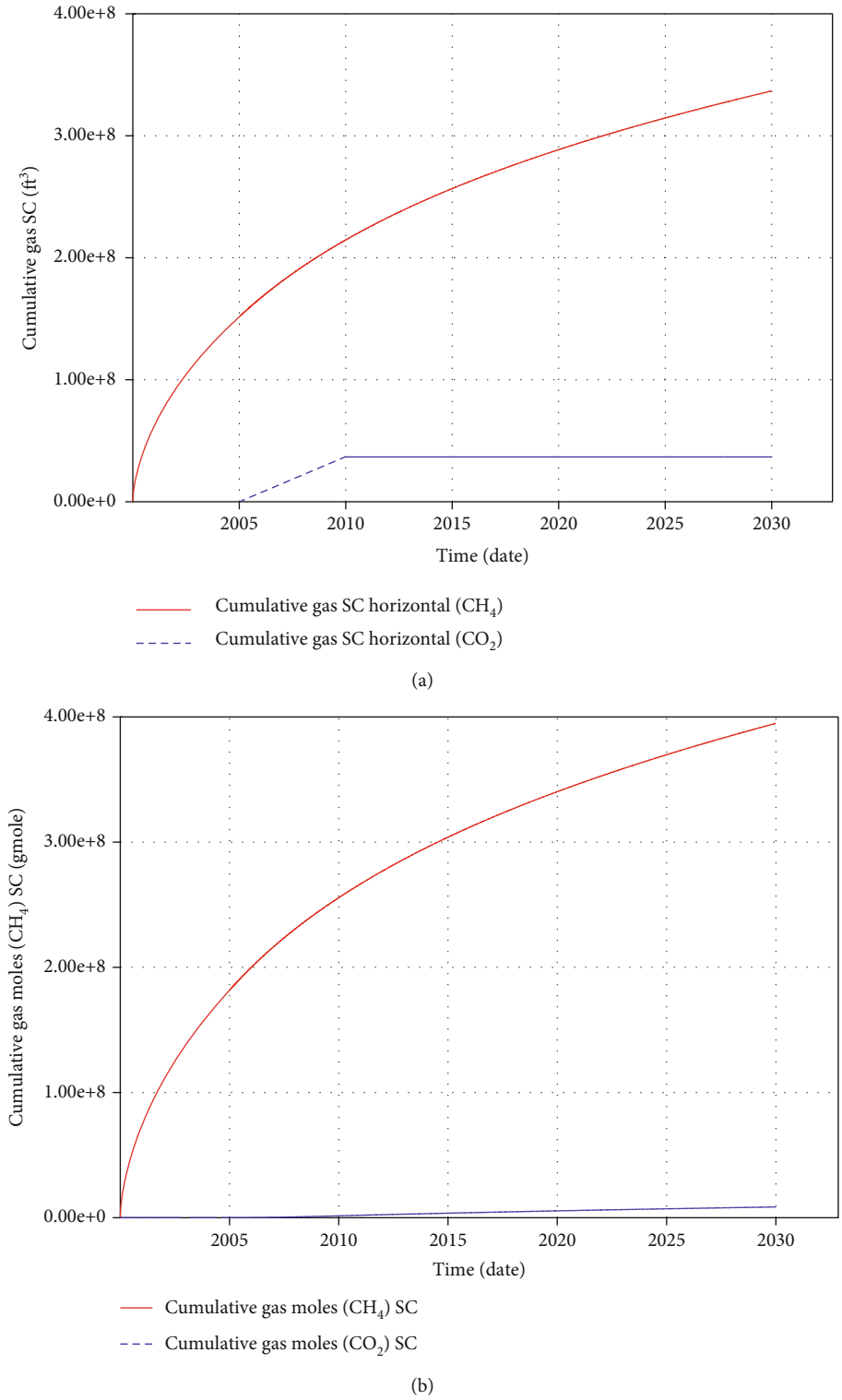

Figure 7: (a) Simulation results of scheme 3: cumulative gas production, CO_2 injection; (b) cumulative production of each component.

supplemental energy is trapped around an injector, which cannot be fully harnessed for efficient development, as shown in Figure 6(b). Meanwhile, the cumulative injection of CO_2 is halved for the pulse injection, which reduces its impact on produced natural gas purity, resulting in higher CH_4 production in scheme 3 compared to scheme 2. The simulation results of the three schemes are summarized in Table 2.

2.5. Sensitivity Analysis of Interfracture Reservoir Permeability. Yu et al. [29] conducted a sensitivity analysis

Table 2: Simulation results of three schemes.

Scheme	Cumulative gas production (10^6 m^3)	Total gas injection (10^6 m^3)	CH_4 production (10^6 m^3)	CO_2 production (10^6 m^3)	CO_2 sequestration ratio (%)
Depletion development	9.52	—	9.52	—	—
Continuous injection	9.56	2.07	9.31	0.25	87.9
Pulse injection	9.53	1.04	9.33	0.20	80.8

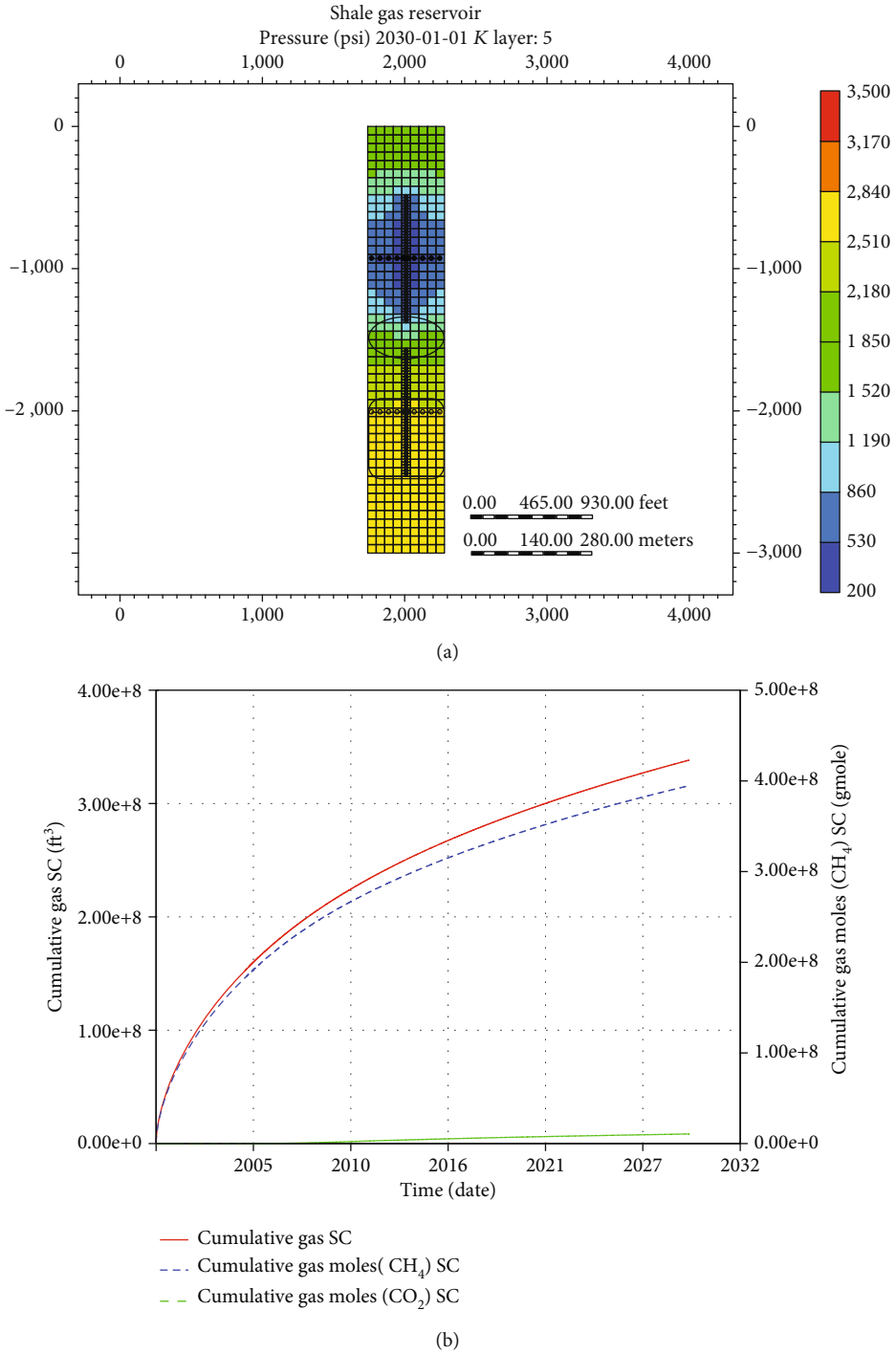

Figure 8: (a) Pressure distribution of scheme 2.1; (b) cumulative gas production, cumulative CH_4, CO_2 production.

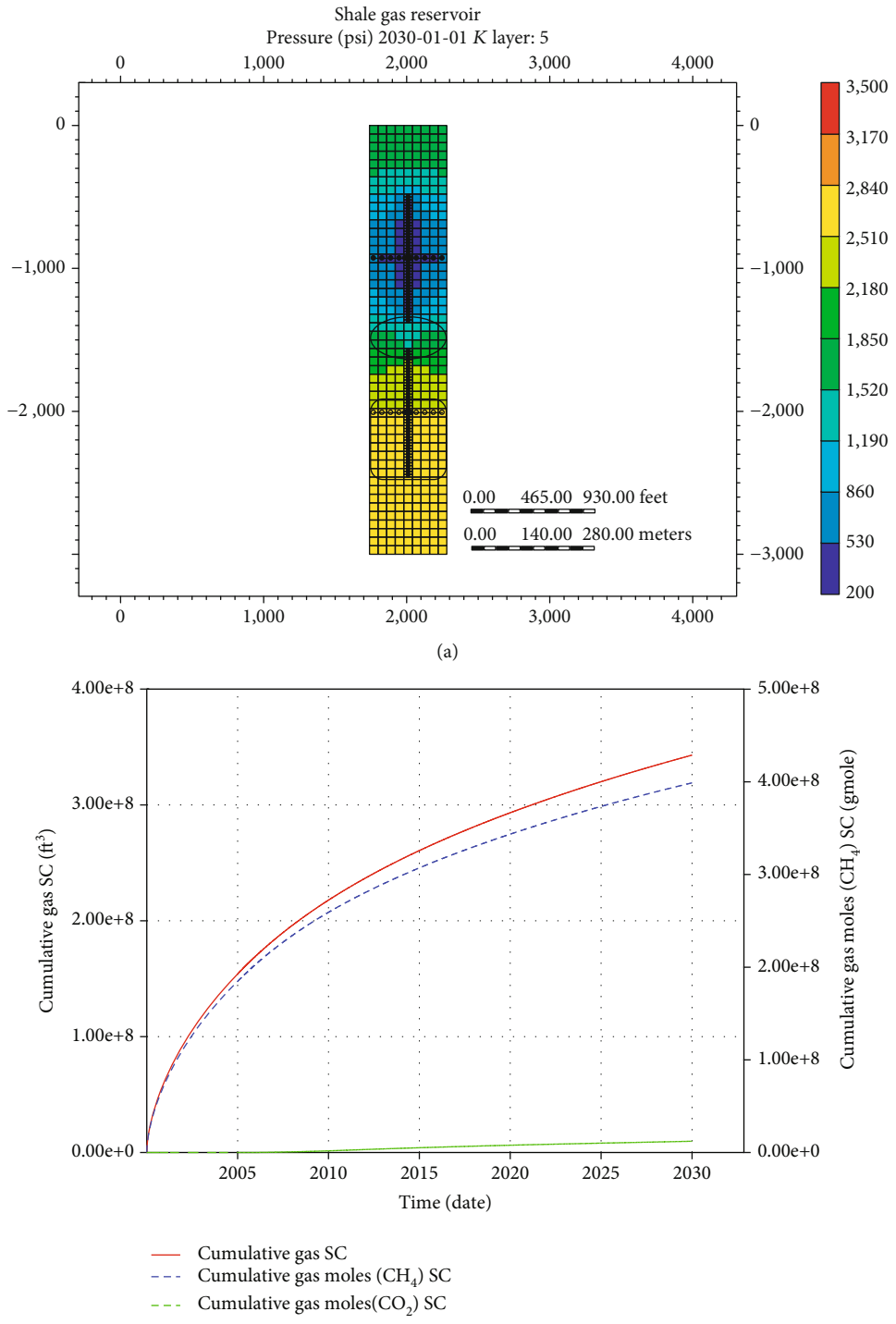

Figure 9: (a) Pressure distribution of scheme 2.2; (b) cumulative gas production, cumulative CH_4, CO_2 production.

on the primary factors affecting shale gas development with CO_2 injection. Among them, reservoir permeability has the greatest impact on reservoir performance. Based on the above numerical simulation results, it can be observed that the tight and unstimulated shale matrix between the hydraulic fractures of the producer and injector seriously affects the energy transfer efficiency, resulting in the inefficient development of shale gas. Therefore, the sensitivity analysis of interfracture reservoir permeability (reservoir permeability between the hydraulic fractures of the producer and injector) is carried out to further explore and quantify the potential of the shale gas reservoir performance with the CO_2 injection. The spacing between the hydraulic fractures of the producer and injector is 55 m.

On the basis of scheme 2, three subschemes are established: scheme 2.1 increases the interfracture permeability

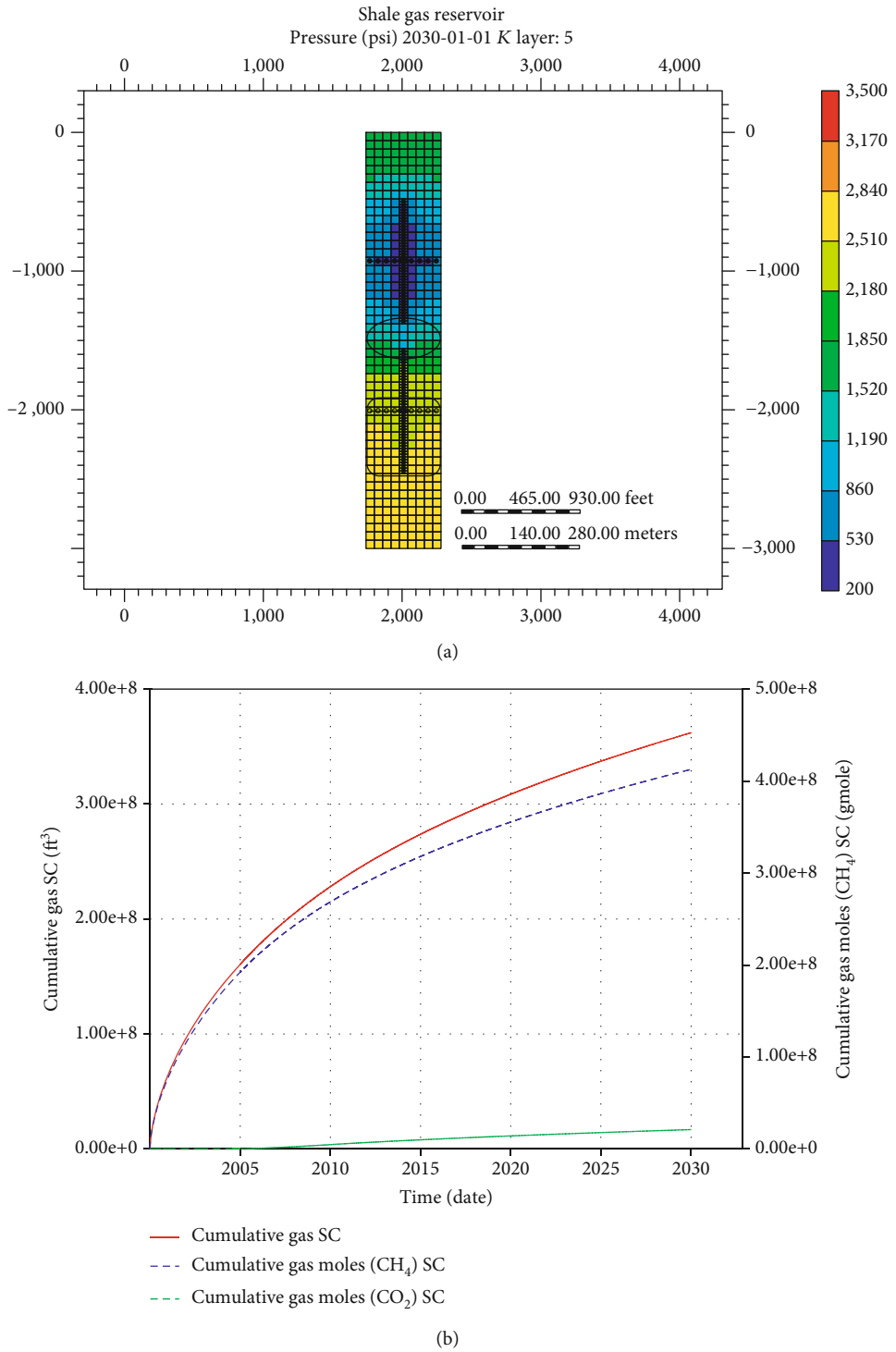

Figure 10: (a) Pressure distribution of scheme 2.3; (b) cumulative gas production, cumulative CH_4, CO_2 production.

to 10 times of the original permeability, scheme 2.2 increases to 100 times, and scheme 2.3 increases to 1000 times. Here, scheme 2 is set as a benchmark for the three subschemes. With the outcomes of simulation (Figures 8–10), it is found that under the same gas injection volume as scheme 2, the total gas production of scheme 2.1 is $9.58 \times 10^6\ m^3$, which is increased by 0.21% compared with scheme 2. CH_4 production is $9.33 \times 10^6\ m^3$, increased by 0.21%; CO_2 production is $0.25 \times 10^6\ m^3$, increased by 1.08%. Scheme 2.2 total gas production is $9.71 \times 10^6\ m^3$, increased by 1.57%; the CH_4 production is $9.42 \times 10^6\ m^3$, increased by 1.18%. CO_2 production is $0.29 \times 10^6\ m^3$, increased by 16%. Scheme 2.3 total gas production is $10.25 \times 10^6\ m^3$, increased by 7.21%; CH_4 production is $9.75 \times 10^6\ m^3$, increased by 4.73%; CO_2 production is $0.50 \times 10^6\ m^3$, increased by 100.56%. Based on the above numerical experiments, in a word, the bigger

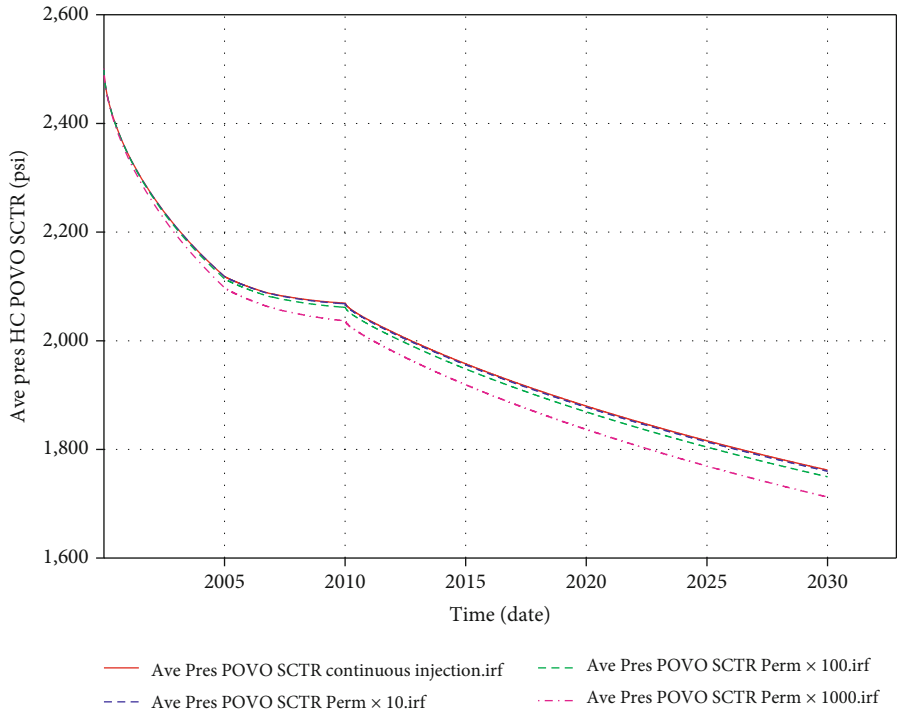

Figure 11: Reservoir average pressure evolution of scheme 2.1, scheme 2.2, and scheme 2.3.

Table 3: Simulation results of scheme 2.1, scheme 2.2, and scheme 2.3.

Permeability multiples	Cumulative gas production (10^6 m^3)	Total gas injection (10^6 m^3)	CH_4 production (10^6 m^3)	CO_2 production (10^6 m^3)	CO_2 sequestration ratio (%)
10	9.58	2.07	9.33	0.25	87.9
100	9.71	2.07	9.42	0.29	86.0
1,000	10.25	2.07	9.75	0.50	75.8

the interfracture permeability is, the better the reservoir performance is. Due to the increase of interfracture permeability, the pressure transmits easier from the injector to the producer (Figure 11). The efficiency of supplemental energy utilization is improved, and the average pressure of the whole reservoir declines faster, which is the main reason for the increase in CH_4 production. The finding indicates that energy utilization efficiency plays a key role in improving shale gas recovery by CO_2 injection. Otherwise, the supplemental energy will not be effectively harnessed to benefit the reservoir development. The pressure status of the grid blocks, which is highlighted in Figures 8–10, also indicates that the producer of the case with bigger interfracture permeability exhibits higher energy utilization efficiency in the drainage area. In other words, an effective pressure-driven system between the injector and producer is established and more supplemental energy is utilized to benefit the recovery process for the case with bigger interfracture permeability. Meanwhile, not only CH_4 production has increased, but also CO_2 production has increased significantly with the increase of interfracture permeability (Table 3), which is harmful to the sequestration of CO_2 in shale reservoirs. In order to meet the demand for both CO_2 sequestration and EGR, it is essential to establish effective communication between the injector and producer via fracking, which is beneficial to efficient energy transmission. Meanwhile, the communication between the injector and producer should be appropriate to prevent CO_2 from channeling, which is beneficial to the effective sequestration of CO_2. The successful CO_2 interwell flooding strategy in shale reservoirs for the sequestration process sets higher requirements for on-site fracking operations. A moderate secondary stimulation zone needs to be formed between the primary hydraulic fractures of the injector and producer to facilitate the efficient energy transfer between interwell as well as to prevent CO_2 from channeling, such as scheme 2.3. Before the field pilot, it is necessary to take the efficiency of supplemental energy utilization, the CO_2 sequestration ratio, and the effect of injected CO_2 on the purity of produced methane into consideration to design an optimal execution plan.

3. Conclusions

In this paper, with the data from the New Albany Shale reservoir in the Illinois Basin, the CMG-GEM simulator is implemented to establish a numerical model to evaluate the feasibility of CO_2 sequestration in shale gas reservoirs with potential enhanced gas recovery (EGR). With the established

shale reservoir model, different CO_2 injection schemes (continuous injection vs. pulse injection) for CO_2 sequestration in shale gas reservoirs are investigated. Meanwhile, a sensitivity analysis of the reservoir permeability between the hydraulic fractures of production and injection wells is conducted to quantify its influence on reservoir performance. Based on the above research, the following conclusions are obtained:

(1) CO_2 sequestration in shale gas reservoirs is technically feasible. With appropriate well spacing and effective stimulation, the gas production is improved by the injection of carbon dioxide which also lowers the purity of produced natural gas

(2) Due to the tight and unstimulated matrix between the hydraulic fractures of the injector and producer, the pressure transfer efficiency of both continuous injection and pulse injection is low, which leads to the inefficient development of shale gas. But the injected CO_2 is effectively sequestered. The tight interfracture formation acts as a double-edged sword here. The tight interfracture formation reduces the energy transfer efficiency, which dominates the success of the EGR. Meanwhile, the tight interfracture formation effectively prevents CO_2 from channeling, which benefits CO_2 sequestration in shale. In the field application, it is necessary to take the efficiency of supplemental energy utilization, the CO_2 sequestration ratio and the effect of injected CO_2 on the purity of produced methane into consideration to design an optimal execution plan

(3) Based on the sensitivity analysis of interfracture reservoir permeability conducted to quantify its influence on reservoir performance, the success of the EGR is determined by the energy transfer efficiency between the injector and producer. Meanwhile, with the increase of the interfracture reservoir permeability, the CO_2 sequestration ratio decreases. In order to meet the demand for CO_2 sequestration in shale gas reservoirs with EGR, advanced and effective fracking is essential, which means that a moderate secondary stimulation zone needs to be formed between the primary hydraulic fractures of injection and production wells to facilitate efficient energy transfer between interwell as well as to prevent CO_2 from channeling, such as scheme 2.3

Data Availability

Data is available upon request.

Conflicts of Interest

The authors declare no conflict of interest.

Authors' Contributions

Conceptualization was performed by J.Z.; methodology was performed by J.Z. and X.M.; software was performed by J.Z., Z.N., and Y.Z.; investigation was performed by J.Z., M.L., and R.W.; writing (original draft preparation) was performed by J.Z.; writing (review and editing) was performed by J.Z., C.F., and Z.N.; funding was acquired by J.Z. and X.M.

Acknowledgments

The School of Petroleum Engineering at Xi'an Shiyou University is highly appreciated. This research is supported by the General Project of National Natural Science Foundation of China (Grant No. 51974253), the Youth Project of National Natural Science Foundation of China (Grant No. 52004219), the Scientific Research Program Funded by Shaanxi Provincial Education Department (Grant No. 20JS117), the Natural Science Foundation of Shaanxi Province (Grant Nos. 2020JQ-781 and 221717005), the Open Fund of State Key Laboratory of Shale Oil and Gas Enrichment Mechanisms and Effective Development (Grant No. G5800-20-ZS-KFGY018), and the Open Fund of State Key Laboratory of Oil and Gas Reservoir Geology and Exploitation (Southwest Petroleum University) (Grant No. PLN2021-12).

References

[1] S. C. Peter, "Reduction of CO2to chemicals and fuels: a solution to global warming and energy crisis," *ACS Energy Letters*, vol. 3, no. 7, pp. 1557–1561, 2018.

[2] M. I. Qureshi, A. M. Rasli, and K. Zaman, "Energy crisis, greenhouse gas emissions and sectoral growth reforms: repairing the fabricated mosaic," *Journal of Cleaner Production*, vol. 112, pp. 3657–3666, 2016.

[3] M. Höök and X. Tang, "Depletion of fossil fuels and anthropogenic climate change–a review," *Energy Policy*, vol. 52, pp. 797–809, 2013.

[4] S. Bachu and J. J. Adams, "Sequestration of CO_2 in geological media in response to climate change: capacity of deep saline aquifers to sequester CO_2 in solution," *Energy Conversion and Management*, vol. 44, no. 20, pp. 3151–3175, 2003.

[5] R. P. Hepple and S. M. Benson, "Geologic storage of carbon dioxide as a climate change mitigation strategy: performance requirements and the implications of surface seepage," *Environmental Geology*, vol. 47, no. 4, pp. 576–585, 2005.

[6] W. Zhang, Y. Li, T. Xu, H. Cheng, Y. Zheng, and P. Xiong, "Long-term variations of CO_2 trapped in different mechanisms in deep saline formations: a case study of the Songliao Basin, China," *International Journal of Greenhouse Gas Control*, vol. 3, no. 2, pp. 161–180, 2009.

[7] K. S. Lackner, "Climate change: a guide to CO_2 sequestration," *Science*, vol. 300, no. 5626, pp. 1677-1678, 2003.

[8] J. D. Figueroa, T. Fout, S. Plasynski, H. McIlvried, and R. D. Srivastava, "Advances in CO_2 capture technology–the U.S. Department of Energy's Carbon Sequestration Program," *International Journal of Greenhouse Gas Control*, vol. 2, no. 1, pp. 9–20, 2008.

[9] Z. Dai, H. Viswanathan, R. Middleton et al., "CO_2 accounting and risk analysis for CO_2 sequestration at enhanced oil recovery sites," *Environmental Science & Technology*, vol. 50, no. 14, pp. 7546–7554, 2016.

[10] F. A. Rahman, M. M. A. Aziz, R. Saidur et al., "Pollution to solution: capture and sequestration of carbon dioxide (CO_2)

and its utilization as a renewable energy source for a sustainable future," *Renewable and Sustainable Energy Reviews*, vol. 71, pp. 112–126, 2017.

[11] M. Mukherjee and S. Misra, "A review of experimental research on enhanced coal bed methane (ECBM) recovery via CO_2 sequestration," *Earth-Science Reviews*, vol. 179, pp. 392–410, 2018.

[12] J. Zhan, Z. X. Chen, Y. Zhang, Z. G. Zheng, and Q. Deng, "Will the future of shale reservoirs lie in CO_2 geological sequestration?," *SCIENCE CHINA Technological Sciences*, vol. 63, no. 7, pp. 1154–1163, 2020.

[13] J. Zhan, Q. Yuan, A. Fogwill et al., "A systematic reservoir simulation study on assessing the feasibility of CO_2 sequestration in shale gas reservoir with potential enhanced gas recovery," in *Carbon Management Technology Conference*, Houston, Texas, USA, 2017.

[14] J. Zhan, E. Soo, A. Fogwill et al., "A systematic reservoir simulation study on assessing the feasibility of CO_2 sequestration in liquid-rich shale gas reservoirs with potential enhanced gas recovery," in *Offshore Technology Conference Asia*, Kuala Lumpur, Malaysia, 2018.

[15] B. C. Nuttal, C. Eble, R. M. Bustin, and J. A. Drahovzal, "Analysis of Devonian black shales in Kentucky for potential carbon dioxide sequestration and enhanced natural gas production," in *Greenhouse Gas Control Technologies 7*, Elsevier Science Ltd, 2005.

[16] S. M. Kang, E. Fathi, R. J. Ambrose, I. Y. Y. Akkutlu, and R. F. F. Sigal, "Carbon dioxide storage capacity of organic-rich shales," *SPE Journal*, vol. 16, no. 4, pp. 842–855, 2011.

[17] M. Godec, G. Koperna, R. Petrusak, and A. Oudinot, "Potential for enhanced gas recovery and CO_2 storage in the Marcellus Shale in the eastern United States," *International Journal of Coal Geology*, vol. 118, pp. 95–104, 2013.

[18] J. Zhang, *Study on Adsorption and Desorption of Continental Shale Gas in Fuxian District*, Southwest Petroleum University, Ordos Basin, 2013.

[19] K. Zhang, J. Xie, C. Li, L. Hu, X. Wu, and Y. Wang, "A full chain CCS demonstration project in northeast Ordos Basin, China: operational experience and challenges," *International Journal of Greenhouse Gas Control*, vol. 50, pp. 218–230, 2016.

[20] D. Dong, C. Zou, J. Dai et al., "Suggestions on the development strategy of shale gas in China," *Journal of Natural Gas Geoscience*, vol. 1, no. 6, pp. 413–423, 2016.

[21] D. Liu, *Study on the CO_2 Enhanced Shale Gas Recovery Technology in Ordos Basin*, China University of Geosciences, 2017.

[22] C. Zhang, *Research on the Feasibility of CO_2 Enhanced Shale Gas Recovery*, Tsinghua University, 2015.

[23] F. Liu, K. Ellett, Y. Xiao, and J. A. Rupp, "Assessing the feasibility of CO_2 storage in the New Albany Shale (Devonian-Mississippian) with potential enhanced gas recovery using reservoir simulation," *International Journal of Greenhouse Gas Control*, vol. 17, pp. 111–126, 2013.

[24] Z. Chen, *Reservoir Simulation: Mathematical Techniques in Oil Recovery*, Society for Industrial and Applied Mathematics, 2007.

[25] CMG, *GEM User's Guide*, Computer Modelling Group Ltd, 2015.

[26] R. D. Evans and F. Civan, *Characterization of Non-Darcy Multiphase Flow in Petroleum Bearing Formation. Final Report*, Oklahoma Univ. School of Petroleum and Geological Engineering, Norman, OK (United States), 1994.

[27] B. Rubin, "Accurate simulation of Non-Darcy flow in stimulated fractured shale reservoirs," in *SPE Western regional meeting*, Anaheim, California, USA, 2010.

[28] A. Novlesky, A. Kumar, and S. Merkle, "Shale gas modeling workflow: from microseismic to simulation–a Horn River case study," in *Canadian Unconventional Resources Conference*, Calgary, Alberta, Canada, 2011.

[29] W. Yu, E. W. Al-Shalabi, and K. Sepehrnoori, "A sensitivity study of potential CO_2 injection for enhanced gas recovery in Barnett shale reservoirs," in *SPE unconventional resources conference*, The Woodlands, Texas, USA, 2014.